

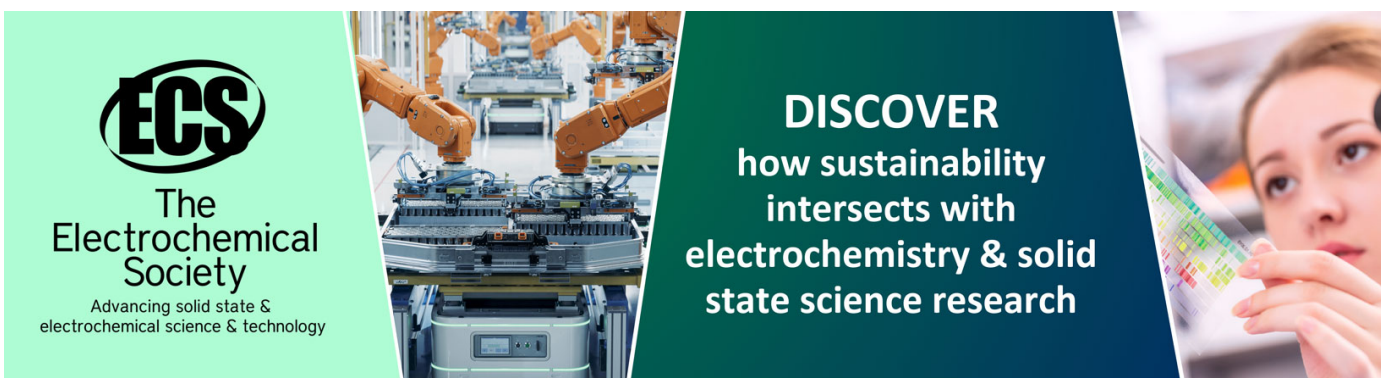
Multiferroic and magnetoelectric properties of $\text{Bi}_{1-x}\text{Ba}_x\text{Fe}_{1-x}\text{Mn}_x\text{O}_3$ system

To cite this article: L H Yin *et al* 2009 *J. Phys. D: Appl. Phys.* **42** 205402

View the [article online](#) for updates and enhancements.

You may also like

- [Characterization of the \$\text{La}_{1-x}\text{Ba}_x\text{CoO}_3\$ \(\$0 < x < 1\$ \) System as Cathode Material for IT-SOFC](#)
C. Setevich, L. Mogni, A. Caneiro *et al.*
- [Optical and Structural Properties of \$\text{Eu}^{2+}\$ -doped \(\$\text{Sr}_{1-x}\text{Ba}_x\$ \) \$_2\text{SiO}_4\$ phosphors](#)
Jong Su Kim, Yun Hyung Park, Jin Chul Choi *et al.*
- [Active and passive defects in tetragonal tungsten bronze relaxor ferroelectrics](#)
Bi-Xia Wang, M J Krogstad, H Zheng *et al.*



ECS
The
Electrochemical
Society
Advancing solid state &
electrochemical science & technology

DISCOVER
how sustainability
intersects with
electrochemistry & solid
state science research

Multiferroic and magnetoelectric properties of $\text{Bi}_{1-x}\text{Ba}_x\text{Fe}_{1-x}\text{Mn}_x\text{O}_3$ system

L H Yin¹, W H Song^{1,4}, X L Jiao², W B Wu², X B Zhu¹, Z R Yang¹,
J M Dai¹, R L Zhang³ and Y P Sun^{1,4}

¹ Key Laboratory of Materials Physics, Institute of Solid State Physics, and High Magnetic Field Laboratory, Chinese Academy of Sciences, Hefei 230031, People's Republic of China

² Hefei National Laboratory for Physics Sciences at the Microscale, University of Science and Technology of China, Hefei 230026, People's Republic of China

³ Ningbo Institute of Material Technology and Engineering, Chinese Academy of Sciences, Ningbo 315040, People's Republic of China

E-mail: whsong@issp.ac.cn and ypsun@issp.ac.cn

Received 29 June 2009, in final form 11 August 2009

Published 23 September 2009

Online at stacks.iop.org/JPhysD/42/205402

Abstract

Multiferroic compounds $\text{Bi}_{1-x}\text{Ba}_x\text{Fe}_{1-x}\text{Mn}_x\text{O}_3$ ($0.2 \leq x \leq 0.5$) have been synthesized by conventional solid-state reaction. X-ray diffraction shows that $\text{Bi}_{1-x}\text{Ba}_x\text{Fe}_{1-x}\text{Mn}_x\text{O}_3$ is single phase up to $x = 0.4$. These samples exhibit magnetism and ferroelectricity simultaneously at room temperature. A considerable enhancement of the polarization on magnetic poling and a dielectric anomaly near the magnetic transition (T_C) due to the intrinsic magnetoelectric coupling effect are observed in the $\text{Bi}_{0.8}\text{Ba}_{0.2}\text{Fe}_{0.8}\text{Mn}_{0.2}\text{O}_3$ sample. The dielectric constant for the $\text{Bi}_{0.8}\text{Ba}_{0.2}\text{Fe}_{0.8}\text{Mn}_{0.2}\text{O}_3$ sample at room temperature decreases with increasing applied magnetic fields, and the coupling coefficient $(\varepsilon'(H) - \varepsilon'(0))/\varepsilon'(0)$ reaches -0.2% at $H = 6 \text{ kOe}$.

(Some figures in this article are in colour only in the electronic version)

1. Introduction

Multiferroic materials that simultaneously show electric and magnetic orderings have recently attracted a considerable surge of attention due to the promising multifunctional device applications and underlying new physics [1–3]. The coupling between magnetic and ferroelectric (FE) degrees of freedom in multiferroics can produce a number of interesting phenomena, such as the magnetoelectric (ME) effect, in which the magnetization can be tuned by the applied electric fields and vice versa [1–3]. One of the most widely investigated multiferroics is BiFeO_3 (BFO) due to its FE and magnetic transition temperatures locating well above room temperature (RT), giving rise to possibilities of RT multiferroic devices [4]. BFO has a rhombohedrally distorted perovskite structure in the space group $R3c$ at RT with a FE Curie temperature of

$\sim 1100 \text{ K}$ [5]. The ferroelectricity in BFO is believed to be due to the Bi 6s lone pair electrons [6], while the magnetism is thought to originate from the partially filled d orbitals of Fe. It is a G-type antiferromagnet (AFM) ($T_N \sim 643 \text{ K}$) with a spatially modulated spiral spin structure [7, 8]. This spiral spin structure can be suppressed or even destroyed by applying high magnetic fields [9], chemical substitutions [10] or epitaxial strain [11], etc. Recently, considerable effort has been made to get both strong FE and ferromagnetic (FM) polarization and/or a large ME effect at RT through A-site and/or B-site doping in ABO_3 -type perovskite BFO [10, 12–14]. However, numerous problems still need to be resolved to achieve the aim of getting a large enough RT ME effect for practical application, one of which is that special conditions, such as high pressure, are required for the synthesis of the Bi-based perovskites [15]. Recently, we note that it has been suggested that Ba doping in BFO could effectively suppress the spiral spin structure, and, in fact, the appearance

⁴ Authors to whom any correspondence should be addressed.

of net magnetization at RT has been observed [10]. On the other hand, various studies have suggested that the statistical distribution of Fe^{3+} ions with 4+ ions in the octahedra or the creation of lattice defects can lead to bulk magnetization and ferromagnetism [16, 17]. The aforementioned points have motivated us to try to (1) synthesize the compounds at normal conditions through conventional and simple routes; (2) suppress the spiral spin structure of BFO and get strong FM interaction between B-site elements; (3) keep FE properties and get large ME effects at RT through A-site and B-site co-doping. Based on these considerations, we have synthesized the $\text{Bi}_{1-x}\text{Ba}_x\text{Fe}_{1-x}\text{Mn}_x\text{O}_3$ ($0.2 \leq x \leq 0.5$) compounds and exploited the possibility of multiferroic features. In this work, the synthesis and structure of the $\text{Bi}_{1-x}\text{Ba}_x\text{Fe}_{1-x}\text{Mn}_x\text{O}_3$ ($0.2 \leq x \leq 0.5$) compounds, and the multiferroic and ME properties of the representative sample, i.e. $\text{Bi}_{0.8}\text{Ba}_{0.2}\text{Fe}_{0.8}\text{Mn}_{0.2}\text{O}_3$, are presented.

2. Experimental

Polycrystalline $\text{Bi}_{1-x}\text{Ba}_x\text{Fe}_{1-x}\text{Mn}_x\text{O}_3$ ($0.2 \leq x \leq 0.5$) samples were prepared by a conventional solid-state reaction method from high purity Bi_2O_3 , Fe_2O_3 , MnO_2 and BaCO_3 . The stoichiometric powders were mixed thoroughly, placed into Al_2O_3 crucibles and then fired in air at 750°C for 24 h. The resultant powders were ground, pressed into small pellets and sintered at 850°C for 24 h and finally at 900°C for another 24 h with an intermediate grinding.

The RT x-ray diffraction (XRD) measurements were taken by a Philips X'pert PRO x-ray diffractometer with $\text{Cu } K_\alpha$ radiation. The XRD data were analysed by the Rietveld method [18] with Rietica [19]. The direct current (dc) resistance as a function of temperature was measured by the standard four-probe method. Dielectric measurements were performed using an LCR meter in the frequency range 1 kHz–1 MHz at temperatures ranging from RT to 700 K. RT FE hysteresis loops were measured by using a TF Analyzer 2000 (aixACCT) at a frequency of 1 kHz. The magnetic measurements were carried out from RT to 800 K using a vibrating sample magnetometer (VSM) (Quantum Design PPMS system) fitted with a high temperature oven option.

3. Results and discussions

From RT XRD studies (see figure 1(a)), we find that $x = 0.2$ and 0.4 samples are single phase crystallizing in the same structure as the BFO compound, and some extra peaks attributed to the impurities are observed for the sample $x = 0.5$. Good agreement between the observed and calculated diffraction patterns is obtained for $x \leq 0.4$ samples in the $R3c$ space group-based model and the Rietveld analysis results for $x = 0.2$ are shown in figure 1(b). The structural parameters are refined by the standard Rietveld technique [18]. Ba and Mn substitution with $x \leq 0.4$ has not affected the crystalline structure of the parent compound BFO, which is important for the FE properties of the compounds. However, Ba and Mn substitution leads to a decrease in the unit cell volume from 371.86 \AA^3 for $x = 0.2$ to 370.03 \AA^3 for $x = 0.4$.

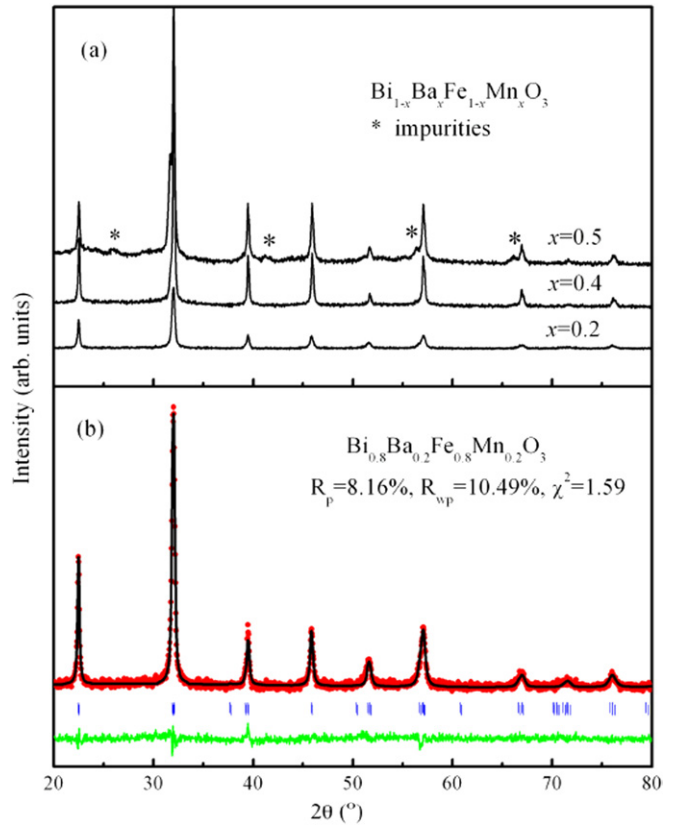


Figure 1. (a) RT XRD patterns of the $\text{Bi}_{1-x}\text{Ba}_x\text{Fe}_{1-x}\text{Mn}_x\text{O}_3$ ($0.2 \leq x \leq 0.5$) samples, “*” indicates the presence of impurity phases. (b) Rietveld analysis results of XRD pattern at RT for the $\text{Bi}_{0.8}\text{Ba}_{0.2}\text{Fe}_{0.8}\text{Mn}_{0.2}\text{O}_3$ sample. Solid circles indicate the experimental data and the continuous line overlapping them. The lowest curve shows the difference between experimental and calculated patterns. The vertical bars indicate the Bragg reflection positions; $R_p = 8.16\%$, $R_{wp} = 10.49\%$ and $\chi^2 = 1.59$.

This decrease in unit cell volume with increasing Ba and Mn substitution and the decrease in unit cell volume for the $\text{Bi}_{0.8}\text{Ba}_{0.2}\text{Fe}_{0.8}\text{Mn}_{0.2}\text{O}_3$ sample in comparison with that of $\text{Bi}_{0.8}\text{Ba}_{0.2}\text{FeO}_3$ (378.90 \AA^3) [20] are expected since the ionic radius of Mn^{4+} is slightly smaller than that of Fe^{3+} . This reduction in lattice parameters indirectly confirms the existence of Mn^{4+} in the sample.

Figure 2(a) shows the temperature dependence of the magnetization (M) of the $\text{Bi}_{0.8}\text{Ba}_{0.2}\text{Fe}_{0.8}\text{Mn}_{0.2}\text{O}_3$ sample measured in the mode of zero field cooling (ZFC) and field cooling (FC) at a magnetic field of 1 kOe. The magnetic transition temperature (T_C) calculated from the minimum position of the dM/dT versus temperature curve (see the inset of figure 2(a)) is around 660 K. In order to study the ME coupling between the FE and magnetic orders, we also measured the dielectric constant (ϵ') in the temperature range from RT to 700 K in a frequency range 1–1000 kHz. The measured result is plotted in figure 2(b). It is obvious that an anomaly in $\epsilon'(T)$ can be observed near the magnetic transition temperature T_C similar to that observed in other multiferroics [21, 22]. This anomaly in $\epsilon'(T)$ near T_C is more clearly shown in the inset of figure 2(a) at a selected frequency of 10 kHz. Generally, such an anomaly in $\epsilon'(T)$

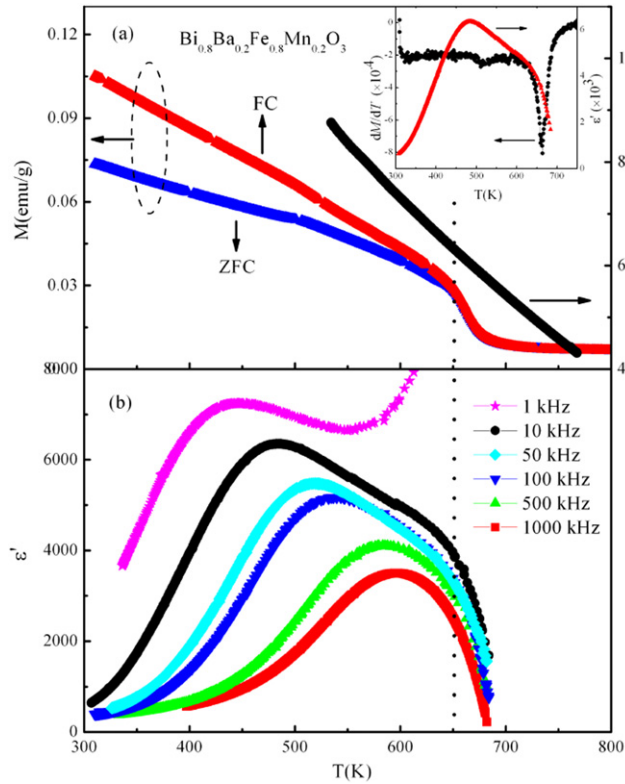


Figure 2. (a) Temperature dependence of magnetization for ZFC and FC modes measured at 1 kOe and dc resistance for the $\text{Bi}_{0.8}\text{Ba}_{0.2}\text{Fe}_{0.8}\text{Mn}_{0.2}\text{O}_3$ sample. (b) Temperature dependence of the real part of dielectric constant at various measuring frequencies for the $\text{Bi}_{0.8}\text{Ba}_{0.2}\text{Fe}_{0.8}\text{Mn}_{0.2}\text{O}_3$ sample. The inset in (a) shows (dM/dT) versus temperature plot for FC magnetization and $\epsilon'(T)$ across T_C at 10 kHz.

may originate from different factors, such as an extrinsic resistive component of the dielectric response together with the Maxwell–Wagner effect [23], which can lead to an artefact in the dielectric enhancement produced by the carrier migration to the interfaces within any heterogeneous semiconductor, and intrinsic multiferroic coupling via the magnetoelastic effect [22, 24]. To verify the origin of the anomaly in $\epsilon'(T)$ observed in the $\text{Bi}_{0.8}\text{Ba}_{0.2}\text{Fe}_{0.8}\text{Mn}_{0.2}\text{O}_3$ sample, the temperature dependence of dc resistance across T_C was also measured, as shown in figure 2(a). It shows that no anomaly can be observed in the dc resistance near T_C , compared with the distinct anomaly in $\epsilon'(T)$ near T_C , implying that the role of the resistive part of the dielectric response is insignificant. This helps us to exclude the possibility of the resistive origin of the dielectric anomaly near T_C . On the other hand, lattice distortion and unit cell parameter anomalies have been observed at the magnetic transition temperature in BFO based solid solutions [22] and YMnO_3 [24]. Based on these facts we can attribute the anomaly in $\epsilon'(T)$ near T_C to the intrinsic ME coupling in the $\text{Bi}_{0.8}\text{Ba}_{0.2}\text{Fe}_{0.8}\text{Mn}_{0.2}\text{O}_3$ sample.

In addition to the anomaly in $\epsilon'(T)$ near T_C , an obvious dielectric relaxation below T_C can also be observed in the dielectric spectra (see figure 2(b)) of the $\text{Bi}_{0.8}\text{Ba}_{0.2}\text{Fe}_{0.8}\text{Mn}_{0.2}\text{O}_3$ sample. The temperature (T_m) corresponding to the peak in $\epsilon'(T)$ shows considerable frequency dispersion. It shifts from 440 K at 1 kHz to 596 K at

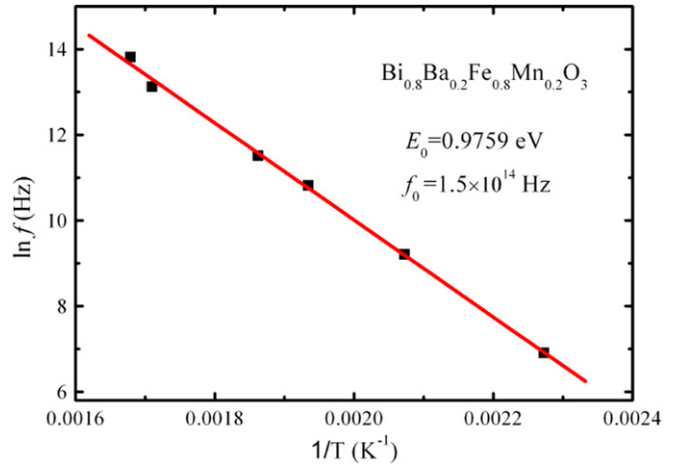


Figure 3. Temperature of dielectric constant maximum as a function of ac frequency for the $\text{Bi}_{0.8}\text{Ba}_{0.2}\text{Fe}_{0.8}\text{Mn}_{0.2}\text{O}_3$ sample. Squares are experimental points and solid line is Arrhenius law fitting.

1 MHz on increasing the measuring frequency, accompanied by the decrease in the peak value of the dielectric constant at T_m . This behaviour is similar to that observed in relaxor ferroelectrics [25, 26]. However, the frequency dependent T_m does not obey the Vogel–Fulcher relation

$$f = f_0 \exp(-E_0/k_B(T_m - T_f)) \quad (1)$$

observed in canonical relaxor ferroelectrics [24], but obeys the Arrhenius relation

$$f = f_0 \exp(-E_0/k_B T_m). \quad (2)$$

Here f is the measured alternating-current (ac) frequency, k_B is the Boltzmann constant, T_f is the finite temperature at which the relaxor dynamics ‘freeze’ into a polarizable state, f_0 is a prefactor and E_0 is the activation energy. This Arrhenius relation can be clearly seen in figure 3 which depicts the $\ln f$ versus $1/T$ plot. The fitting parameters thus obtained are $E_0 = 0.9759$ eV and $f_0 = 1.5 \times 10^{14}$ Hz. This activation energy (0.9759 eV), comparable to 1.26 eV for $\text{Sr}(\text{Fe}_{1/2}\text{Nb}_{1/2})\text{O}_3$ [27], is very close to the activation energy (~ 1 eV) for the motion of oxygen vacancies. This indicates that the dielectric relaxation below T_C has a close relation to the defect ordering in the sample.

Figure 4 shows the magnetization hysteresis loop ($M-H$) of the $\text{Bi}_{0.8}\text{Ba}_{0.2}\text{Fe}_{0.8}\text{Mn}_{0.2}\text{O}_3$ sample measured at 300 K, which indicates a weak ferromagnetism existing in the sample. This hysteresis loop cannot be attributed to the possible presence of impurity phases such as $\text{Bi}_2\text{Fe}_4\text{O}_9$ with the magnetic transition temperature around 260 K [28]. However, according to Goodenough–Kanamori rules [29], a FM interaction should appear between the e_g electrons of the $\text{Fe}^{3+}(d^5)$ and the t_{2g} electrons of the $\text{Mn}^{4+}(d^3)$, whereas a strong AFM interaction is expected between Fe ions. As mentioned above, the Mn^{4+} ions indeed exist in our samples, which might be the cause of the appearance of RT magnetic hysteresis loops. On the other hand, it has been suggested that the spatially modulated spiral spin structure of BFO can be suppressed by doping [20, 30]. Hence, it is expected that the spiral spin

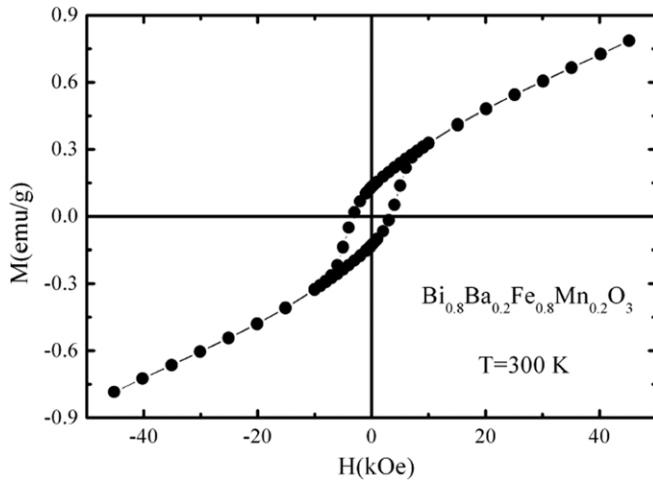


Figure 4. Magnetic hysteresis loop $M(H)$ measured at 300 K for the $\text{Bi}_{0.8}\text{Ba}_{0.2}\text{Fe}_{0.8}\text{Mn}_{0.2}\text{O}_3$ sample.

structure might be suppressed or even destroyed and hence the net magnetization could appear in the $\text{Bi}_{1-x}\text{Ba}_x\text{Fe}_{1-x}\text{Mn}_x\text{O}_3$ solid solution system.

Figure 5(a) shows the RT capacitance versus voltage curve ($C-V$), using an applied voltage of 5 V. A typical butterfly-shaped loop, as seen in the $C-V$ curve, is observed, implying a signature of FE behaviour at RT in the sample [31]. The RT polarization–electric field ($P-E$) measurement at a frequency of 1 kHz for the $\text{Bi}_{0.8}\text{Ba}_{0.2}\text{Fe}_{0.8}\text{Mn}_{0.2}\text{O}_3$ sample reveals both a FE and a leaky behaviour of the sample, which is shown in figure 5(b). At the maximum applied electric field of $\pm 0.42 \text{ kV cm}^{-1}$, the remanent polarization (P_r) is about $0.023 \mu\text{C cm}^{-2}$. A fully saturated hysteresis loop could not be obtained due to the leaky nature of the sample.

To further demonstrate the coupling between electric and magnetic polarizations, the effects of magnetic poling on the FE hysteresis loop and the dielectric constant at a frequency of 10 kHz as a function of the applied magnetic field measured at 300 K are plotted in figures 5(b) and 6. After poling the sample at a dc magnetic field of 70 kOe for 30 min, the FE hysteresis loop showed considerable enhancement in the remanent polarization from 0.023 to $0.057 \mu\text{C cm}^{-2}$. The variation of the dielectric constant as a function of the applied magnetic field, i.e. $(\epsilon'(H) - \epsilon'(0))/\epsilon'(0)$, is commonly used to describe the ME coupling in multiferroics [32, 33]. The dielectric constant ϵ' decreases with increasing applied magnetic field in the $\text{Bi}_{0.8}\text{Ba}_{0.2}\text{Fe}_{0.8}\text{Mn}_{0.2}\text{O}_3$ sample, giving the largest negative coupling coefficient of -0.2% at the highest magnetic field of 6 kOe. This value is larger than that of Nb [34] or Mn [13] doped BiFeO_3 but smaller than that of Tb doped BiFeO_3 [14]. It should be noted that the magnetocapacitance can also be influenced by the magnetoresistance (MR) effect as suggested by Catalan [22]. To see the influence of MR on the magnetodielectric effect observed in figure 6, we studied the variation in MR with the magnetic field up to 6 kOe. We did not observe any change in the MR with the increase in the magnetic field up to 6 kOe. Therefore, the magnetodielectric effect is expected to be an intrinsic effect of the sample. The ME coupling observed in our sample could be qualitatively

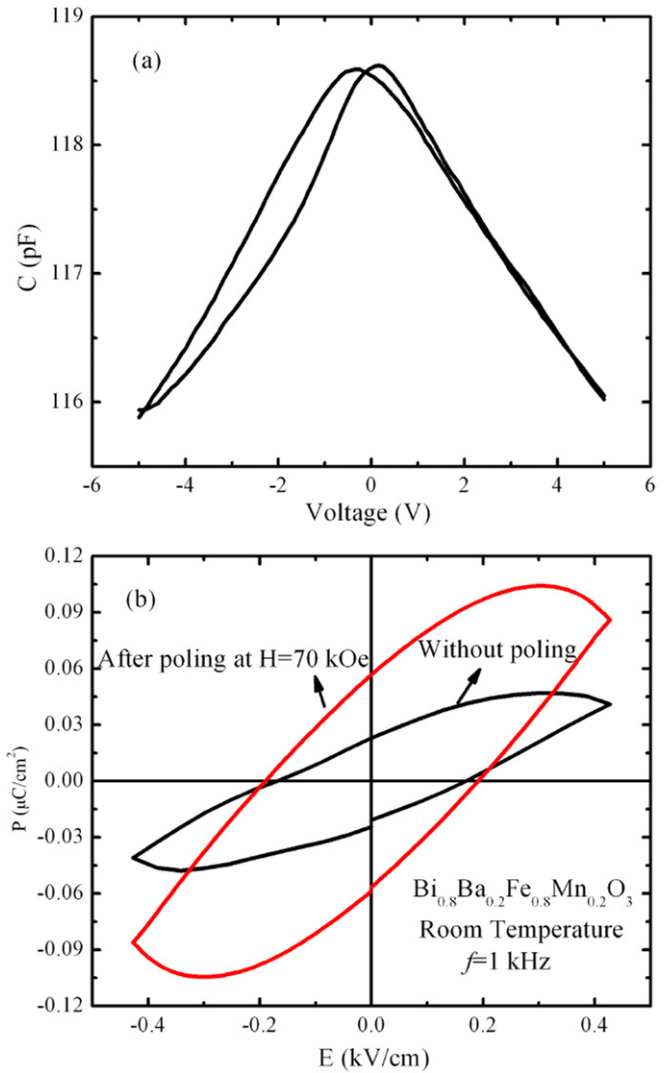


Figure 5. (a) Capacitance versus voltage ($C-V$) butterfly loop measured at RT for the $\text{Bi}_{0.8}\text{Ba}_{0.2}\text{Fe}_{0.8}\text{Mn}_{0.2}\text{O}_3$ sample. (b) RT polarization–electric field hysteresis loop $P(E)$ measured at a frequency of 1 kHz before and after poling at a dc magnetic field of 70 kOe for the $\text{Bi}_{0.8}\text{Ba}_{0.2}\text{Fe}_{0.8}\text{Mn}_{0.2}\text{O}_3$ sample.

understood as follows. When a magnetic field is applied to a multiferroic material, the material will be strained. Due to the coupling between the magnetic and FE domains [35], the strain would induce a stress and then generate an electric field. This field could orient the FE domains, leading to the increase in the polarization value and the change in the dielectric constant [14].

4. Conclusions

In summary, an anomaly is observed in the dielectric constant $\epsilon'(T)$ near T_C due to the intrinsic ME coupling in the $\text{Bi}_{0.8}\text{Ba}_{0.2}\text{Fe}_{0.8}\text{Mn}_{0.2}\text{O}_3$ sample. In addition, a dielectric relaxation below T_C is found to obey the Arrhenius law, which is suggested to originate from the defect ordering. The increase in the remanent polarization after poling in the magnetic field and the decrease in the dielectric constant with increasing applied magnetic fields indicate ME coupling between

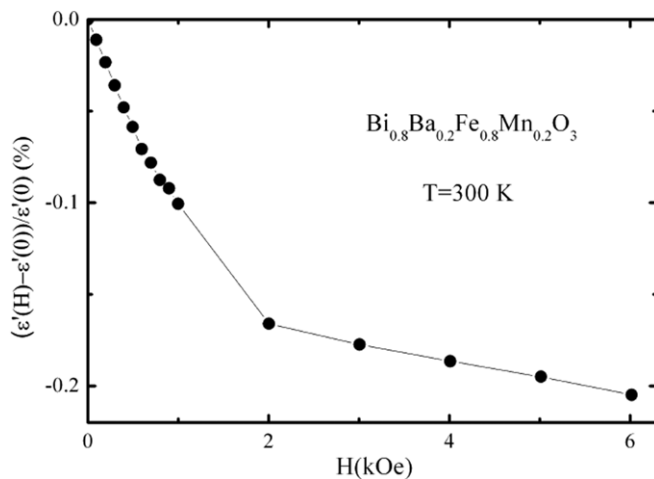


Figure 6. Dielectric constant versus applied magnetic fields curve measured at RT for the $\text{Bi}_{0.8}\text{Ba}_{0.2}\text{Fe}_{0.8}\text{Mn}_{0.2}\text{O}_3$ sample.

magnetic and electric dipoles in the $\text{Bi}_{0.8}\text{Ba}_{0.2}\text{Fe}_{0.8}\text{Mn}_{0.2}\text{O}_3$ sample at RT. It is significant that the coexistence of magnetic and electric orderings at RT in the $\text{Bi}_{0.8}\text{Ba}_{0.2}\text{Fe}_{0.8}\text{Mn}_{0.2}\text{O}_3$ sample makes it a potential candidate for device applications.

Acknowledgments

This work was supported by the National Key Basic Research under Contract No 2007CB925001, the National Science Foundation (NSF) of China under Contract Nos 50672099, 10874166, 10874051, Anhui Provincial NSF Grant No 070416233 and Zhejiang Provincial NSF Grant No Y606831.

References

- [1] Prellier W, Singh M P and Murugavel P 2005 *J. Phys.: Condens. Matter* **17** R803
- [2] Eerenstein W, Mathur N D and Scott J F 2006 *Nature* **442** 759
- [3] Ramesh R and Spaldin N A 2007 *Nature Mater.* **6** 21
- [4] Bibes M and Barthélemy A 2008 *Nature Mater.* **7** 425
- [5] Teague J R, Gerson R and James W J 1970 *Solid State Commun.* **8** 1073
- [6] Seshadri R and Hill N A 2001 *Chem. Mater.* **13** 2892
- [7] Sosnowska I, Neumair T P and Steichele E 1982 *J. Phys. C: Solid State Phys.* **15** 4835
- [8] Kaczmarek W, Pajak Z and Polomska M 1975 *Solid State Commun.* **17** 807
- [9] Ruetter B, Zvyagin S, Pyatakov A P, Bush A, Li J F, Belotelov V I, Zvezdin A K and Viehland D 2004 *Phys. Rev. B* **69** 064114
- [10] Wang D H, Goh W C, Ning M and Ong C K 2006 *Appl. Phys. Lett.* **88** 212907
- [11] Wang J *et al* 2003 *Science* **299** 1719
- [12] Yu B F, Li M Y, Wang J, Pei L, Guo D Y and Zhao X Z 2008 *J. Phys. D: Appl. Phys.* **41** 185401
- [13] Yang C H, Koo T Y and Jeong Y H 2005 *Solid State Commun.* **134** 299
- [14] Palkar V R, Kundaliya D C, Malik S K and Bhattacharya S 2004 *Phys. Rev. B* **69** 212102
- [15] Suchomel M R, Thomas C I, Allix M, Rosseinsky M J and Fogg A M 2007 *Appl. Phys. Lett.* **90** 112909
- [16] Gehring G A 1994 *Ferroelectrics* **161** 275
- [17] Goodenough J B and Longo 1978 *LB Series* vol III/4a (New York: Springer)
- [18] Mccusker L B, Von Dreele R B, Cox D E, Louër D and Scandi P 1999 *J. Appl. Crystallogr.* **32** 36
- [19] Hunter B A and Howard C J *Rietica* (available from www.ccp14.ac.uk)
- [20] Khomchenko V A, Shvartsman V V, Borisov P, Kleemann W, Kiselev D A, Bdikin I K, Vieira J M and Kholkin A L 2009 *J. Phys. D: Appl. Phys.* **42** 045418
- [21] Kumar M and Yadav K L 2007 *J. Appl. Phys.* **101** 054105
- [22] Singh A, Pandey V, Kotnala R K and Pandey D 2008 *Phys. Rev. Lett.* **101** 247602
- [23] Catalan G 2006 *Appl. Phys. Lett.* **88** 102902
- [24] Lee S *et al* 2008 *Nature* **451** 805
- [25] Bokov A A and Ye Z G 2006 *J. Mater. Sci.* **41** 31
- [26] Samara G A 2003 *J. Phys.: Condens. Matter* **15** R367
- [27] Liu Y Y, Chen X M, Liu X Q and Li L 2007 *Appl. Phys. Lett.* **90** 192905
- [28] Singh A K, Kaushik S D, Kumar Brijesh, Mishra P K, Venimadhav A, Siruguri V and Patnaik S 2008 *Appl. Phys. Lett.* **92** 132910
- [29] Goodenough J B 1955 *Phys. Rev.* **100** 564
- [30] Sosnowska I, Schäfer W, Kockelmann W, Andersen K H and Troyanchuk I O 2002 *Appl. Phys. A: Mater. Sci. Process. A* **74** S1040
- [31] Uchida N and Ikeda T 1965 *Japan. J. Appl. Phys.* **4** 867
- [32] Kimura T, Kawamoto S, Yamada Y, Azuma M, Takano M and Tokura Y 2003 *Phys. Rev. B* **67** 180401(R)
- [33] Kimura T, Goto T, Shinatani H, Ishizaka K, Arima T and Tokura Y 2003 *Nature* **426** 55
- [34] Jun Y K, Moon W T, Chang C M, Kim H S, Ryu H S, Kim J W, Kim K H and Hong S H 2005 *Solid State Commun.* **135** 133
- [35] Fiebig M, Lottermoser T, Frohlich D, Goltsev A V and Pisarev R V 2002 *Nature* **419** 818